J Solid State Eletrochem (2004) 8: 330–336
DOI 10.1007/s10008-003-0457-x

ORIGINAL PAPER

Nijole Dukstiene · Kiril Kazancev · Igoris Prosicevas
Asta Guobiene

Electrodeposition of Mo-Se thin films from a sulfamatic electrolyte

Received: 27 April 2003 / Accepted: 19 September 2003 / Published online: 8 November 2003

Abstract Mo-Se thin films have been electrodeposited on conducting tin oxide (SnO_2) coated glass substrates from a sulfamatic solution containing Na_2MoO_4 and H_2SeO_3 under potentiostatic conditions. The deposition potential varied from −0.6 V to −0.9 V, at a deposition temperature of 20–40 °C and pH 6.5. X-ray diffraction analysis revealed that the overall composition of the films deposited is consistent with the formation of MoO_2 and $MoSe_2$. The lattice parameters of the "as-deposited" $MoSe_2$ are $a = b = 3.2340$ Å and $c = 13.2859$ Å, which fits a hexagonal structure.

Keywords Electrodeposition · Molybdenum · Selenium · Thin films

Introduction

Molybdenum diselenide absorbs in the visible and near-IR regions and exhibits an inherent resistive nature to photocorrosion [1]. $MoSe_2$ has a layered sandwich structure and the layers of Se-Mo-Se interact with each other by van der Waals forces, which allow adjacent layers to slide. It is easy for ions such as Li^+ or Na^+ to intercalate in the interlayer gaps, due to a large *d*-spacing between two layers. All these properties cause layered $MoSe_2$ to have special applications in precursors for intercalation superconductors [2], materials for photoelectrochemical cells [3, 4] and solid-state lubricants.

N. Dukstiene (✉) · K. Kazancev
Department of Physical Chemistry,
Kaunas University of Technology,
Radvilienu pl. 19,
3028 Kaunas, Lithuania
E-mail: nijole.dukstiene@ktu.lt

I. Prosicevas · A. Guobiene
Institute of Physical Electronics,
Kaunas University of Technology,
Savanoriu pr. 271,
3009 Kaunas, Lithuania

Traditionally, crystalline molybdenum diselenide has been synthesized by a solid-state reaction between a stoichiometric amount of elemental molybdenum and selenium in a sealed evacuated tube at a temperature of at least 900 °C for several days [5]. A metathetical reaction between high-valent molybdenum halides and alkali-metal selenides proceeds rapidly and yields the crystalline product. This reaction is known as a self-propagating high-temperature synthesis (SHS) [6]. A similar reaction between molybdenum halides and alkali-metal selenides in organic solvents has also been explored [7] to produce amorphous $MoSe_2$ at room temperature.

As a developing synthetic technology, solvothermal synthesis has gained much attention. It is generally conducted at intermediate temperatures (100–400 °C) in a sealed system. Nanocrystalline 2H-$MoSe_2$ has been prepared from MoO_3, $N_2H_4{\cdot}H_2O$ and Se in pyridine at 300 °C for 12 h by the solvothermal method [8]. However, these high-temperature methods suffer from the difficulty of producing large amounts of material and are expensive. The high production cost of such materials requires the search for a cheaper method. These techniques include electrodeposition and chemical deposition.

The preparation of transition metal chalcogenide thin films by electrodeposition methods is currently attracting considerable attention, as it is relatively inexpensive, simple and convenient for large area preparations [9, 10]. In electrochemistry, to our knowledge, only one experimental study has been made [11] and only for one type of $MoSe_2$ sample. A highly textured $MoSe_2$ film with a polycrystalline nature has been electrodeposited from an ammoniacal solution of H_2MoO_4 and SeO_2 under potentiostatic conditions. The electrode potential was fixed at −0.9 V_{SCE}. The bath temperature was maintained at 40 °C. The structure and properties of the thin films are strongly dependent on the electrodeposition conditions. Hence, the present paper concerns the influence of the experimental conditions (temperature, potential applied, bath composition) on the structure, composition and

morphology of Mo-Se deposits correlated with the appearance and growth of the layer.

Experimental

The study of the electrodeposition mechanism was performed using cyclic voltammetry (CV). The CV experiments were conducted in a thermostat-controlled conventional three-electrode JSE-2 cell with a PI-I-50 potentiostat coupled to a PR-8 programmer and an XY potentiometer recorder (Zip, Russia). Cyclic voltammograms were carried out at a sweep rate of 50 mV s^{-1}, with the potential scanned first in the negative (cathodic) direction.

The working electrode was a conducting tin oxide (SnO_2) coated glass substrate. The geometrical area of the electrode was 5.0 cm^2. The conducting SnO_2 coated glasses were cleaned with acetone, then cleaned electrochemically in 0.1 M HNO_3, rinsed with distilled water and dried in an alcoholic vapour [12]. The auxiliary electrode was a platinum wire. A standard $Ag|AgCl|KCl_{sat}$ electrode was used as the reference electrode. The reference electrode tip was placed very close to the cathode surface so that the exact potential at the surface was monitored, unaffected by the solution resistance. All reported values of electrode potentials are expressed relative to the reference electrode used.

The experiments were performed in an electrochemical aqueous bath containing different amounts of Na_2MoO_4 and H_2SeO_3. To prepare electrolyte solutions having relative concentrations of the components, basic solutions of 1 M Na_2MoO_4 and 1 M H_2SeO_3 were first prepared. The different volumes of basic solutions were mixed to give the electrolysis solutions. A 0.1 M $NH_4SO_3NH_2$ solution was used as a supporting electrolyte. The bath pH was maintained 6.5–6.8. Purified water and chemicals of minimum 98% purity were used. The oxygen in the solution was removed by nitrogen bubbling for 15 min.

Thin films were obtained by cathodic electrodeposition under potentiostatic conditions. The thickness and refraction index of the films were measured by a laser ellipsometer (Gaertner L115, Gaertner Scientific, USA) ($\lambda = 632.8$ nm). An atomic force microscope (Nanotop-206, Microtestmashines, Belarus) operating in a contact-state mode was used to investigate the morphology of the surface. It used a silicon cantilever, with a force constant of 5.0 N m^{-1}. The image processing and analysis of the scanning probe microscopy data were performed using a Windows-based program (Surface View, version 1.0).

Optical microscopy was carried out on a computer microscope (Intel QX3, Intel, USA) at a magnification of 60×. Some samples were removed in a reflection mode and some in a through mode, at additional illumination by an intense heat lamp. The program Image Jhttp://rsb.info.nih.gov/ij/download/zips/ij128.zip processed the results.

X-ray diffractometry was carried out under a Brag Brendan circuit on a diffractometer (Dron-3.0, Bourevestnik, Russia) using Cu K_α ($\lambda = 0.154178$ nm) radiation, 30 kV voltage and 20 mA current. The scanning range was $\theta = 0$–35°. The scanning speed was 1° min^{-1}. Results were registered in "in situ" mode by a computer and then processed by the program X-Fithttp://www.ccp14.ac.uk/tutorial/x-fit95/xfit.htm.

The samples were annealed at a 15 °C min^{-1} rate up to 150–300 °C in an inert nitrogen atmosphere and maintained for 1 h. At the end of the heat treatment the samples were slowly cooled to room temperature.

X-ray fluorescence analysis was carried out by an X-ray spectrometer (VRA-20, Germany) by direct radiation of the thin layer so as not to destroy the $MoSe_2$ layers. The conditions of the specimens investigated by the VRA-20 device were the following: a Rh tube anode, 35 kV voltage and 26 mA current. Specimens were revolved in the horizontal plane in order to improve the X-ray signal stability. The calibration curve was formed in the interval of 0.25–1 μg, using for calibration "thin" layers formed from standard solutions on the filter paper. Distribution of Mo and Se on the standard specimen area was monitored by the UV fluorescence mark method. The "thin" layers criteria were kept for concentrations up to 40 μg mm^{-2}. Various measurements were carried out on different regions of the deposited films and the average composition was determined. The calculated analysis error was less than 5%.

Results and discussion

Cyclic voltammetry measurements

The cyclic voltammograms obtained from the electrolyte solutions can provide the basic information about the process under investigation. A cyclic voltammogram for the tin oxide electrode in 0.1 M $NH_4SO_3NH_2$ solution containing Na_2MoO_4 (Fig. 1) shows a cathodic wave from −0.2 V to −0.55 V (c_1) before the current increases rapidly at $E = -0.6$ V. On the return scan from $E = -1.4$ V in the positive direction, an anodic peak (a_1) with peak potential $E_p = -0.22$ V is observed. The experimental data indicate that the thin films could be electrodeposited only at potentials $E \leq -0.6$ V. The "as-obtained" films are dark brown in colour and well adherent to the substrate. The XRD pattern indicates that the peaks belonging to the polycrystalline MoO_2 films are detected for films prepared at potentials more negative that −0.6 V. The preferential orientation is along the (200) plane. For the films electrodeposited at −0.8 V, seven peaks at $2\theta = 26.467$, 37.784, 51.622, 54.131, 56.291, 59.642 and 61.595°, corresponding to interplanar distances of 3.3648, 2.3790, 1.7691, 1.6929, 1.6330, 1.5532 and 1.504 Å, respectively, were observed, which are in good agreement with the PDF values belonging to MoO_2 (PDF 78-1070).

According to the above results, the MoO_2 films can be successfully deposited at potentials $E \leq -0.6$ V. The height of an anodic peak (a_1) increases by increasing the

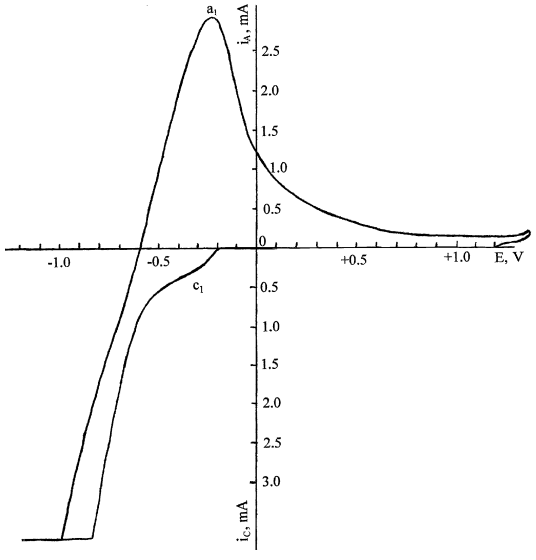

Fig. 1 Cyclic voltammogram for the SnO_2 electrode in an electrolyte containing 0.05 M $Na_2MoO_4 + 0.1$ M $NH_4SO_3NH_2$. Temperature 20 °C; pH 6.5

Na_2MoO_4 content in the electrolyte. Therefore the large anodic peak observed at $E_p = -0.22$ V can be related to the electrooxidation of the deposited MoO_2.

Figure 2 shows the cyclic voltammogram for the tin oxide electrode obtained in 0.1 M $NH_4SO_3NH_2$ solution containing 0.05 M Na_2MoO_4 and 0.01 M H_2SeO. The presence of H_2SeO_3 in the electrolyte bath shifts the cathodic current to the region of more positive potential values (Fig. 1 and Fig. 2). The cathodic wave (c_1) increases in intensity by increasing the H_2SeO_3 content in the electrolyte. On the other hand, the progressive decrease in intensity of the anodic peak (a_1) which is related to the oxidation of MoO_2 and a slight shift of E_p to more negative potentials denotes competition for the deposition sites between MoO_2 and selenium. Besides, the ill-defined anodic (a_2) wave with a potential from $+0.18$ V to $+0.5$ V is usually observed on the cyclic voltammogram. According to the literature data, the oxidation of elemental selenium starts at $E \geq +0.3$ V (SHE) [13]. Since the peak a_2 occurs in the same potential range, it seems plausible to consider that the oxidation of selenium from electrodeposited films occurs at potentials of the anodic peak a_2.

On comparing the successive cyclic voltammograms, it is evident that a simultaneous reduction of MoO_4^{2-} and H_2SeO_3, leading to the formation of Mo-Se thin films, is possible in the same range of cathodic potentials. In the presence of Na_2MoO_4 and H_2SeO_3 a current flow is recorded in the early stages of the cathodic scan (Fig. 2, curve 1). However, the formation of wave c_1 was not accompanied by visible changes of the electrode surface. More precise information on the relation between the electrode potential and the appearance of the electrode surface was obtained in experiments performed at constant potentials. Visual observation performed at constant potentials enabled us to establish that thin film layers are formed at potentials from -0.6 V to -0.9 V. Dark brown films well adherent to the substrate were electrodeposited.

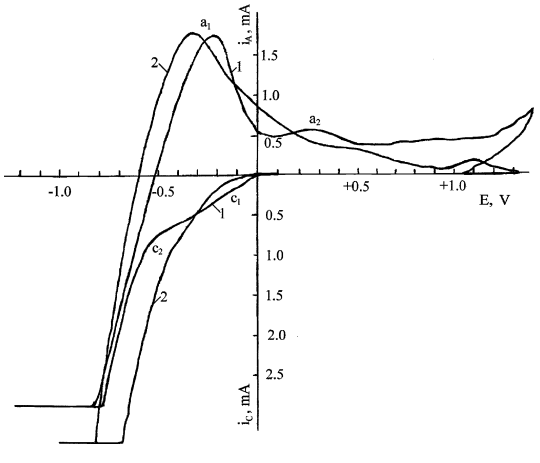

Fig. 2 Cyclic voltammogram for the SnO_2 electrode in various electrolytes: *1*, 0.05 M $Na_2MoO_4 + 0.01$ M $H_2SeO_3 + 0.1$ M $NH_4SO_3NH_2$; *2*, 0.2 M $Na_2MoO_4 + 0.01$ M $H_2SeO_3 + 0.1$ M $NH_4SO_3NH_2$. Temperature 20 °C; pH 6.5

In the usual electrodeposition of metal selenides the Me/Se ratio in the solution should be much larger than unity (≥ 5) [14]. In order to establish the optimum Na_2MoO_4/H_2SeO_3 concentration ratio in the electrodeposition bath, CV experiments were also carried out in solutions containing different amounts of Na_2MoO_4. Typical voltammetric curves illustrating the effect of Na_2MoO_4 concentration are given in Fig. 2. The cathodic current starts immediately below 0.0 V in the electrolyte containing 0.05 M Na_2MoO_4. In solutions containing Na_2MoO_4 at a concentration of 0.2 M the cathodic current flow is recorded at approximately -0.05 V (Fig. 2, curve 2). The anodic peak (a_1) related to the oxidation of MoO_2 in the electrodeposited film shifts to more negative potentials. On the cyclic voltammograms obtained in the electrolyte containing more than 0.2 M Na_2MoO_4, the anodic wave (a_2) assigned to the oxidation of selenium from the electrodeposited film was not detected. These results revealed a prevailing presence of Mo in deposits with the increase of Na_2MoO_4 content in the electrolyte. Thus Na_2MoO_4 concentrations in the bath from 0.05 M to 0.2 M were selected for further experiments.

In order to determine the optimum deposition time, the electrodeposition was performed by varying the deposition time from 10 to 80 min. The electrolytes with various concentrations of Na_2MoO_4 (0.05, 0.10, 0.15 and 0.20 M) at constant 0.01 M H_2SeO_3 concentration were used. The deposition was carried out at different cathodic potentials: $E_d = -0.6$, -0.7, -0.8 V and -0.9 V. In order to illustrate the influence of the deposition time, the films obtained in the above-mentioned conditions were oxidized up to $E = +1.2$ V in the same electrodeposition electrolytes.

The anodic voltammograms for fresh Mo-Se film deposited at $E = -0.6$ V in the electrolyte containing 0.05 M $Na_2MoO_4 + 0.01$ M $H_2SeO_3 + 0.1$ M $NH_3SO_3NH_2$ are presented in Fig. 3, which clearly shows that at constant temperature and Na_2MoO_4/H_2SeO_3 ratio in solution the product of potentiostatic electrolysis at -0.6 V depends upon the electrodeposition time. As can be seen, the anodic voltammograms are significantly affected by the potentiostatic electrolysis time. Almost upon the deposition time of 1 h an anodic current (a_2) related to oxidation of Se is observed (curve 2). At shorter deposition times, peak (a_1) related to the oxidation of MoO_2 is usually seen on the voltammograms. The profiles of all anodic voltammograms for the plated films are similar to those presented in Fig. 3, irrespective of the above-mentioned electrodeposition conditions. It is obvious from the results presented above that the assimilation of Se into the solid phase is sluggish and a deposition-controlled process. The deposits on the conducting SnO_2-coated glass substrate achieve an optimal thickness for the deposition time of 1 h. It is also found that the films are uniform and well adherent to the substrate. It is important to remark that when the thickness exceeded the optimum value, the layers started to peel off from the substrate. This is reasonable if we

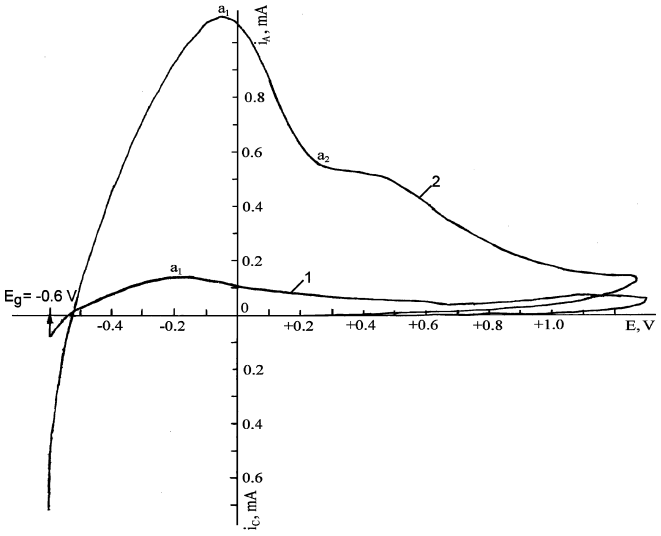

Fig. 3 Anodic striping voltammogram for the Mo-Se thin film deposited on the SnO_2 electrode at $E=-0.6$ V in the electrolyte 0.05 M $Na_2MoO_4+0.01$ M $H_2SeO_3+0.1$ M $NH_4SO_3NH_2$. Deposition time: *1*, 15 min; *2*, 60 min. Temperature 20 °C; pH 6.5

conclude that the optimal deposition time for Mo-Se thin film formation from a sulfamatic electrolyte containing (0.05–0.2 M) $Na_2MoO_4+0.01$ M $H_2SeO_3+0.1$ M $NH_3SO_3NH_2$ is 1 h. Similar results have also been observed by Calixto et al. [15] and Ponamarev et al. [16] for CdTe and MoS_2 electrodeposition, respectively.

Thin film electrodeposition

We examined the electrodeposition of thin film layers under a number of experimental conditions. The film composition and its thickness can be controlled easily by changing the bath composition or electrodeposition conditions. According to the diagnostic test on cyclic voltammograms, the Mo-Se films can be grown at discrete potentials in the range from −0.6 V to −0.9 V and at an optimized deposition time of 1 h.

The temperature of the bath plays an important role in the deposition rate of Mo-Se. The increase of temperature from 20 °C to 60 °C leads to an increase of the electrodeposition growth rate from 203 nm h^{-1} to 884 nm h^{-1}, respectively. When the temperature of the bath is raised above 60 °C, the film growth rate reduces and very thin films were obtained. The films grown were smooth and adhered poorly to the substrate. Such a phenomenon has also been observed in the case of the electrodeposition of WSe_2 thin films [9].

The Mo-Se films obtained in different electrolytes were analyzed for their composition. It was found that the chemical composition of the Mo-Se films depends on the Na_2MoO_4/H_2SeO_3 ratio in the electrolyte. It is interesting to note that the X-ray fluorescence analysis of "as-deposited" films does not confirm the stoichiometry of $MoSe_2$ in the different samples. The XRD analysis allows us to conclude that the overall composition of the deposited films is consistent with the formation of MoO_2 and $MoSe_2$. The chemical composition of films electrodeposited at the deposition potential of −0.8 V is given in Table 1. As seen from this table, the composition of the films changes, depending on the relation of the Na_2MoO_4 and H_2SeO_3 concentrations in the solutions. An increase in the Na_2MoO_4 concentration leads to the enrichment of the deposited layer with MoO_2. These results confirm the cyclic voltammetry data discussed above (Fig. 2).

The "as-deposited" films were characterized by XRD analysis, optical morphology and micro morphology.

XRD analysis

As already evidenced, the constitutional phases of the electrodeposited films are separate $MoSe_2$ and MoO_2. The X-ray diffraction patterns of the "as-deposited" Mo-Se thin film are shown in Fig. 4A. The sharp peaks reveal the polycrystalline nature of the "as-deposited" Mo-Se film. The observed peaks were analyzed to determine the crystal structure of $MoSe_2$ in the film. All the peaks show nearly the same intensity values, confirming the random orientation of the planes in the film. The observed interplaner distance "*d*" values were compared with the standard values (PDF 77-1715) to determine the crystal structure. The structural features fit into a hexagonal lattice with the parameters $a=b=3.2340$ Å and $c=13.2859$ Å.

XRD patterns of the annealed film are shown in Fig. 4B. The lattice parameters of the annealed film are $a=b=3.2815$ Å and $c=13.0095$ Å. There is a very small change in the interplaner distance "*d*" values, but the intensities of the peaks are unaffected for film annealing up to 300 °C. The crystal lattice parameters of the "as-deposited" film and after annealing are in good agreement with the values given in the PDF card (PDF 77-1715). This reveals that the "as-deposited" films are well crystallized.

Table 1 Composition and characterization of samples deposited at different Na_2MoO_4/H_2SeO_3 ratios in the electrolyte. Electrodeposition conditions: $E=-0.8$ V; $T=40$ °C, $\tau=1$ h

Na_2MoO_4/H_2SeO_3 ratio in electrolyte	Film composition (%)		Thickness (nm)	Film characteristic "as deposited"
	MoO_2	$MoSe_2$		
5:1	57.63	42.37	332.0	Brown
10:1	55.95	44.05	386.7	Dark brown
20:1	73.85	26.15	403.8	Dark brown

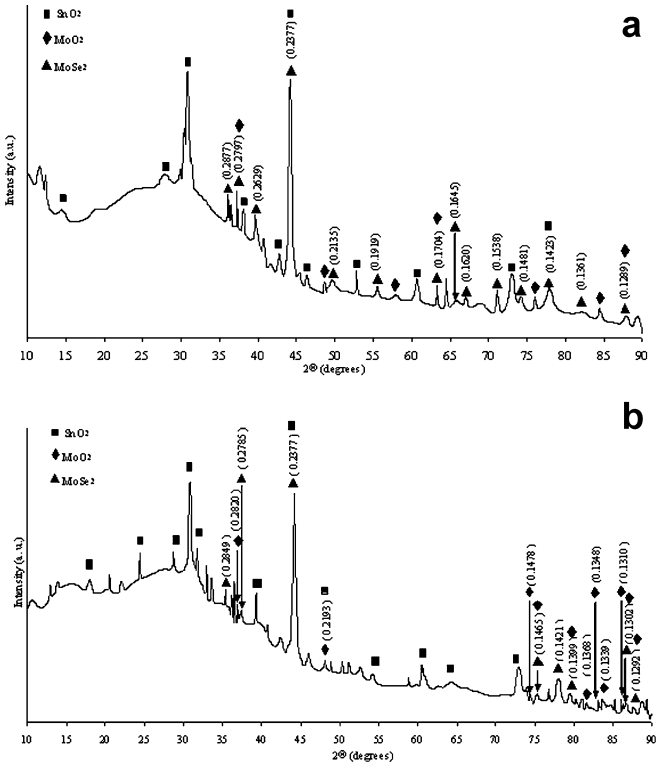

Fig. 4a, b XRD patterns of Mo-Se thin films deposited in the electrolyte 0.05 M $Na_2MoO_4 + 0.01$ M $H_2SeO_3 + 0.1$ M $NH_4SO_3NH_2$. Deposition conditions: $E = -0.6$ V; $T = 20$ °C; pH 6.5; $\tau = 1$ h. **a** "As-deposited". **b** Annealed at 300 °C for 1 h in an inert nitrogen atmosphere

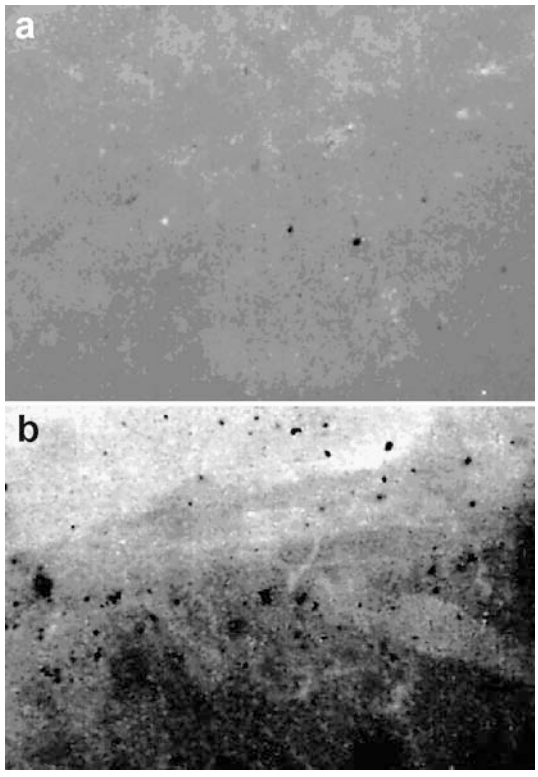

Fig. 5a, b Optical microscope pictures of Mo-Se thin films. **a** "As-deposited". **b** Annealed at 300 °C for 1 h in an inert nitrogen atmosphere

Optical morphology

The optical micrograph of thin Mo-Se films obtained in the electrolyte 0.05 M $Na_2MoO_4 + 0.01$ M $H_2SeO_3 + 0.1$ $NH_4SO_3NH_2$ and deposition potential $E = -0.6$ V is given in Fig. 5A. The micrograph of the surface "as-deposited" Mo-Se layer shows that the film is smooth and homogeneous. The grains size of the film determined by optical microscopy [17] is approximately 30 μm. The fluctuations of sample image optical density along the *x*-axis were in a range from 1.35 up to 164 (at a full scale of optical density from 0 to 255 by the software Image J). The fraction dimension *D* is equal to 1.3034. These results indicate that closely packed grains are uniformly spread over the substrate without any pinholes.

Figure 5B shows the morphology of the annealed film. As can be seen, there are inclusions and uncovered areas. The fraction dimension *D* increased up to 1.6567. The fluctuations of sample image optical density along the *x*-axis were in a range from 0 up to 175. It also confirmed the occurrence of uncovered areas on the SnO_2/glass substrate. The grains size increased up to 50 μm after annealing of the film. These results allow us to conclude that annealing up to 300 °C leads to the destruction of the Mo-Se film

The increase of the Na_2MoO_4 content in the bath leads to the formation of a non-compact film on the substrate. Fine-grained Mo-Se films were also found in this case, but optical microscopy pictures revealed strongly pronounced borders of the grains. The fluctuations of the sample image optical density varied from 5.5 up to 254. Based on the results obtained, it is possible to draw the conclusion that the grains are located at a distance of approximately 2–3 μm apart and do not form a continuous layer. However, these films exhibit good adhesion to the substrate.

An annealing procedure of such films leads to the destruction of the layer. The determined areas of the destroyed film were on average 80 μm. The form of the grains which remained on the SnO_2/glass substrate was irregular with sharp corners.

Micro morphology

The micro morphology of the "as-deposited" and annealed Mo-Se films was studied by AFM. The scanned area was 5 μm×5 μm in all investigations. The "as-deposited" Mo-Se layers were heterogeneity plots and the roughness reached 43.1 nm. The topography and structure of the film layer is clearly seen from the micrographs (Fig. 6A, B and C).

As stated above, the optical microscopy results indicate that annealing of the film leads to destruction of the layer. However, taking into account this phenomenon,

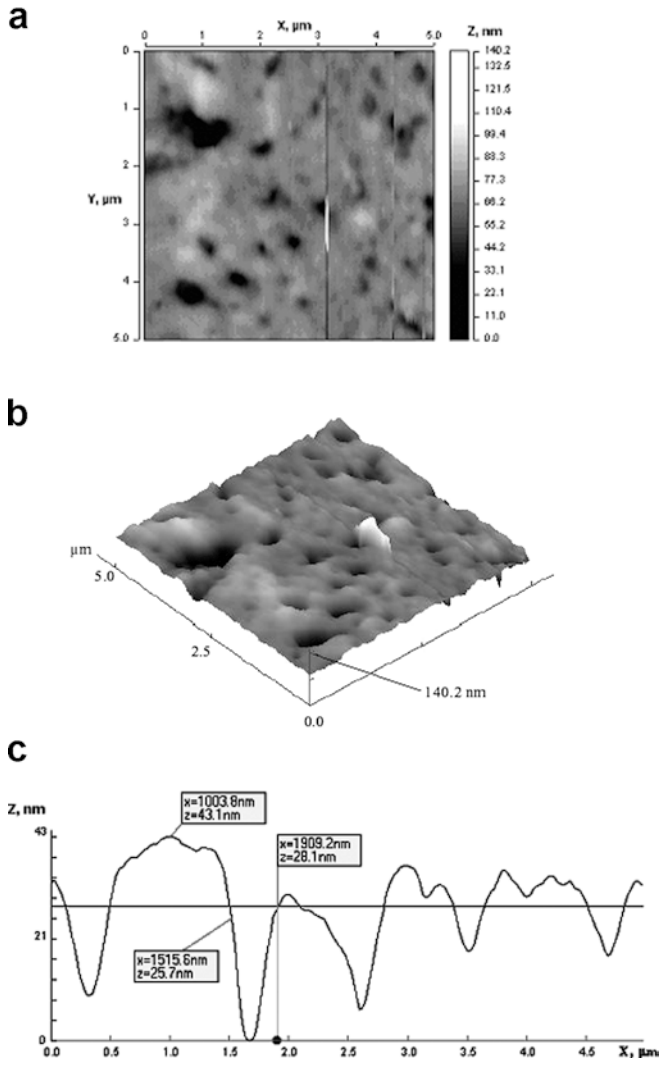

Fig. 6a–c AFM images of the "as-deposited" Mo-Se film layer. Deposition conditions: 0.05 M Na_2MoO_4 + 0.01 M H_2SeO_3 + 0.1 M $NH_4SO_3NH_2$; $E = -0.6$ V; $T = 20$ °C; $\tau = 1$ h. **a** 2D topography. **b** 3D topography. **c** Topography profile

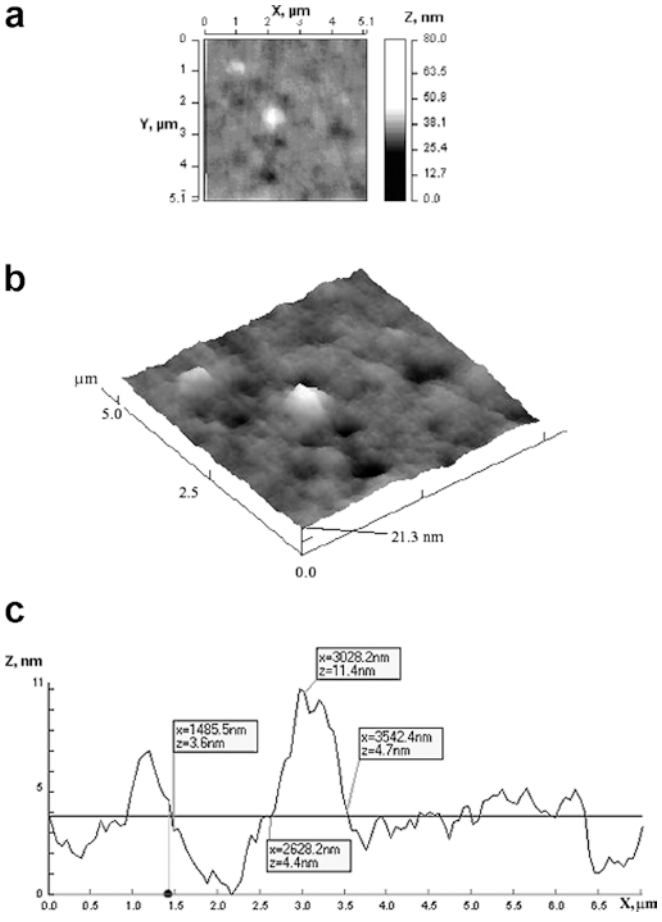

Fig. 7a–c AFM images of the film annealed at 300 °C for 1 h. The Mo-Se film was obtained under the conditions stated in Fig. 6. **a** 2D topography. **b** 3D topography. **c** Topography profile

we examined the influence of annealing on the micro morphology of the films.

To evaluate the influence of annealing on the micro morphology of the films, we analyzed the small areas of the layer which were present on the surface after annealing. The results are shown in Fig. 7. In this particular case, the micrograph of the surface obtained by AFM shows that the small areas of film are uniform, free from pin-holes and adhere well to the substrate (Fig. 7A, B). It is interesting to point out that the annealing of the films influences the roughness of the film surface. The roughness of the annealed films was reduced to 11.4 nm (Fig. 7C).

Conclusions

It has been demonstrated that the electrodeposition of Mo-Se films is possible from a sulfamatic solution containing Na_2MoO_4 and H_2SeO_3. However, it is not possible to avoid the parallel formation of the MoO_2 phase. The global composition of the deposited films is consistent with the presence of $MoSe_2$ and MoO_2. The films are dark brown, very crystalline and adhere well to the substrate. Annealing of the "as-deposited" films leads to destruction of the layer.

Unfortunately, there is still a certain obscurity in the interpretation of the sluggish selenium assimilation into the solid phase and the Mo-Se film formation mechanism. In order to understand this phenomenon, it is important that the electrochemical pathways that occur on the substrate during the Mo-Se film formation are known. It is surprising to note that although considerable work on H_2SeO_3 electroreduction has been done [18, 19, 20, 21, 22, 23, 24, 25], there are no studies devoted to the mechanism of H_2SeO_3 reduction on metal oxide electrodes. Although the successful deposition of $MoSe_2$ has been reported [11], a mechanistic understanding of the deposition process is presently lacking. Through literature reviews it was found that the electrodeposition of Mo in the presence of other metal ions has been referred to as an induced co-deposition mechanism [26, 27, 28].

It is also important to remark that the results presented in this work are consistent with the formation of Mo-Se, but are not conclusive about the reactions and mechanism involved. Analysis of literature data and the experimental results obtained in this work allow us to assume that the formation of Mo-Se could proceed through different routes: by a surface-induced deposition mechanism or a co-deposition mechanism. The possibility of chemical reactions also exists.

Further work seems necessary to better understand selenium assimilation in the solid phase and explain the Mo-Se film formation mechanism. In order to obtain a better insight into the deposition process, a systematic study of the Mo-Se thin film electrodeposition mechanism on a tin oxide electrode is needed. This will be the subject of further studies.

References

1. Pathak VM, Patel KD, Pathak RJ, Srivastva R (2002) Solar Energy Mater Solar Cells 73:117
2. Samoano RB, Rembaum A (1971) Phys Rev Lett 27:402
3. Fan RF, White HS, Wheeler B, Brad AJ (1980) J Electrochem Soc 127:518
4. Schniemeyer LF, Wrighton MS, Stacy A, Siendo MJ (1980) Appl Phys Lett 36:701
5. Woldervanck JC, Jellinek FZ (1964) Z Anorg Allg Chem 328:309
6. Bonneau PR, Jarisis RF, Kaner RB (1997) Nature 349:510
7. Chianelli RR, Dines MB (1978) Inorg Chem 17:2758
8. Zhan JH, Zhang ZD, Qian XF, Wang C, Xie Y, Qian YT (1999) Mater Res Bull 34:497
9. Devadasan J, Jebaraj, Sanjeeisiraja C, Jayachandran M (2002) Mater Chem Phys77:397
10. Patil RS (1999) Thin Solid Films 340:11
11. Anand TJS, Sanjecviraja C, Jayachandran M (2001) Vacuum 60:431
12. Gaikwad NS, Bhosale CH (2002) Mater Chem Phys 76:198
13. Menezes S (1996) Mater Res Soc Symp Proc 426:189
14. Ichimura M, Sato N, Nahamura A, Takencki K, Arai E (2002) Phys Status Solidi A 193:132
15. Calixto ME, McClure JC, Singh VP, Bronson A, Sebastian PJ, Mathew X (2000) Sol Energy Mater Sol Cells 63:325
16. Ponamarev EA, Neumann-Spallart M, Hocks G, Levy-Clement C (1996) Thin Solid Films 280:86
17. Kurzudlowski KJ, Ralph B (1995) Quantitative description of the microstructure of materials. CRC Press, Baton Rouge, USA
18. Jarzabek G, Kublik Z (1980) J Electroanal Chem 114:165
19. Jarzabek G, Kublik Z (1982) J Electroanal Chem 137:247
20. Rao GSR, Reddy S (1985) Acta Chim Hung 118:241
21. Madolo R, Traore M, Vittori O (1986) Electrochim Acta 31:856
22. Mickevicius DL, Dukstiene NV (1990) Chim Lithuan Acad Sci 32:23 (in Russian)
23. Thouin L, Rouquette-Sanchez S, Vedel J (1993) Electrochim Acta 38:2387
24. Massaccen S, Sanchez S, Vedel J (1996) J Electroanal Chem 412:95
25. Kemell M, Saloniemi H, Ritala M, Leskela M (2000) Electrochim Acta 45:3737
26. Salvador P, Chaparro AM, Mir A (1996) J Phys Chem 100:760
27. Castro RJ, Cabrera CR (1997) J Electrochem Soc 144:3135
28. Chaparro AM, Salvador P, Mir A (1997) J Electroanal Chem 424:153